Porosity Evolution of Activated Carbon Fiber Prepared from Liquefied Wood. Part I: Water Steam Activation at 650 to 800 °C

Zhi Jin and Guangjie Zhao*

Activated carbon fiber is known as an excellent adsorbent material due to its well-developed pore structure. In this work, the porosity evolution of activated carbon fiber prepared from phenol liquefied wood with water steam activation at 650 to 800 °C for 20 to 260 min was examined by physical adsorption of N_2 at -196 °C. By the series of activation processes, the specific surface area and pore volume were increased with the increase of activation time, most significantly by activation at 750 °C for 20 to 180 min and by activation at 800 °C for 20 to 260 min. The microporosity was gently and progressively developed with increasing activation time at 650 to 700 °C, while it was sharply developed at the early stage of activations at 750 to 800 °C, and then tended to almost stabilize. The mesoporosity was well developed only by activation at 800 °C for longer than 100 min. The pore size distributions were principally ultramicropores (0.5 - 0.7 nm) during activations at 650 to 700 °C. By activations at 750 to 800 °C, the supermicropores (0.7 to 2.0 nm) as well as mesopores (2 to 4 nm) became progressively more important as the activation time was increased.

Keywords: Liquefied wood-based activated carbon fibers; Porosity evolution; Activation temperature; Activation time

*Contact information: College of Material Science and Technology, Beijing Forestry University, Beijing 100083, China; *Corresponding author: zhaows@bjfu.edu.cn*

INTRODUCTION

Activated carbon fiber (ACF) products are widely used as adsorbents, catalyst supports, capacitors, and for gas storage due to favorable properties such as large specific surface area, high contact efficiency, and light weight (Naik *et al.* 2011). Commonly ACF is produced from polyacrylnitrile, pitch, or rayon. However, such petrochemical products are costly and less environmental friendly. Wood is an abundant and renewable natural resource, which provides energy conservation and reducing costs. Therefore, many studies have been concentrated on the use of wood as a source from which to produce ACF that could replace petrochemicals.

Uraki *et al*. (1997; 2001) studied the ultilization of lignin (the third major component of wood tissue) for preparing ACF. The results showed that acetic acid lignin from hardwood could be easily transformed to fibers by fusion spinning, while acetic acid lignin from softwood could be spun after removing the high-molecular-mass fraction.

Subsequently, these as-spun lignin fibers were converted to carbon fibers by carbonization at 900 to 1000 °C for 0 to 1 h under a nitrogen steam after stabilization (a process to reduce the thermoplasticity by cross-linking and incorporation of oxidized

groups through thermal oxidation at 200 to 300 °C in air) and then activated at 900 °C for 40 to 80 min by introducing steam mixed with nitrogen. The Brunauer-Emmett-Teller (BET) specific surface area (S_{BET}) of the produced ACF reached 1180 to 1930 m^2 g^{-1}, which was comparable to the commercial level of 500 to 2000 m^2 g^{-1} (Qiao *et al.* 2005).

Recently, in order to avoid the difficult separation of wood components and to improve wood utilization, the direct liquefaction process of wood by thermochemical means or with phenol has been applied to acquire liquefied wood (LW) resin that can be spun for ACF manufacture. The resultant ACF also possessed a well-developed pore structure (S_{BET} of 457 - 1645 m^2 g^{-1} following thermo-chemical liquefaction (Qiao *et al.* 2005) and 740 to 2641 m^2 g^{-1} with phenol liquefaction (Liu and Zhao 2012)). Nevertheless, LW by thermochemical means should be produced through a series process consisting of pyrolysis (500 to 750 °C, 12 to 14 °C h^{-1}) of wood and distillation (180 °C for 8 h) of liquid tar (a byproduct from the previous pyrolysis process), while LW with phenol can be obtained only by stirring the mixture of wood and phenol at 160 °C for 2 h with inorganic acid as catalyst. Thus, phenol liquefaction seems to be a simpler process with lower energy cost than thermochemical liquefaction.

It is well known that the pore structure of ACF is greatly influenced by activation temperature and activation time when physical activation with steam is performed. With the increase in activation temperature, steam molecules could react more quickly with active carbon atoms to form more numerous pores, gaps, and cracks, thus increasing the specific surface area in unit weight (Su *et al.* 2012). Moreover, by prolonging the activation time, the pore size distribution (PSD) of ACF will be progressively widened (Kumar *et al.* 1997; Yang and Yu 1998). Thus, various activation degrees controlled by changing activation temperature or activation time allow selection of the ACF porosity. Additionally, the activation process entails the selective removal of carbon, a process that is closely related to the development of porosity as well as the crystal characteristics of the precursor fiber (the fiber before activation). The original gaps and cracks, the lattice defects, and grain boundaries, as well as non-crystalline regions are likely to be activated to generate pores (Osmond 2000; Su *et al.* 2012).

So far, the authors are not aware of any previous report on the porosity evolution of phenol liquefied wood-based ACF (PLWACF) by different activation conditions. Indeed, the application performance of ACF is greatly influenced by its pore structure characteristics. For examples, carbon materials with uniform porosity can be used as molecular sieves for purification process; mesopores (with the pore width of 2 to 50 nm) of 2 to 5 nm in size are superior in constructing electrochemical capacitors; pores at 0.7 to 1.6 nm are beneficial to the methane storage, while the hydrogen storage capacity can be improved by higher amount of micropores (with the pore width smaller than 2 nm) and mesopores less than 6 nm (Im *et al.* 2009; Xu *et al.* 2010; Xie *et al.* 2004; Konwar and De 2013).

Thus, in the present work, PLWACF was prepared with time-consuming activations at different temperature. The evolution of porosity as well as the porosity diversity of PLWACF were investigated. The activation temperature was selected from 650 to 800 °C, because the origin porosity and crystal structure of liquefied wood precursor fiber is known to change greatly within this temperature range (Ma and Zhao 2011; Ma *et al.* 2011).

EXPERIMENTAL

Materials

Wood flour from Chinese fir (*Cunninghamia lanceolata* Lamb.) with 20 to 80 mesh size was dried in an oven at 105 °C for 24 h, and then mixed with phenol. The ratio of wood/phenol was 1/6 by weight. The mixture was added with 8 wt% H_3PO_4 (4.64 mol l^{-1}) as a reaction catalyst and liquefied at 160 °C for 2.5 h with continuous stirring and purified using a sand core funnel (50 mL, 8 cm in diameter) to prepare phenol liquefied wood (PLW). Then 5 wt% hexamethylenetetramine (based on the weight of PLW) was added to the PLW as synthesis agent. The resulted mixture was heated to 175 °C in 40 min and held for 20 min, and then spun at 120 to 130 °C. The resultant fiber was cured by soaking in an acid solution of CH_2O and HCl (37:30 by volume) at 90 °C for 2 h, washed with deionized water, and dried at 85 °C for 2 h. Aliquots of approximately 5 g of the prepared fiber were each heated at a constant rate in a nitrogen stream to 650, 700, 750, and 800 °C, then activated at the corresponding activation temperature for 20, 100, 180 and 240 min by introducing water steam mixed with a nitrogen stream. The resultant PLWACF was cooled to room temperature in a nitrogen stream. The PLWACF samples were noted with "activation temperature (°C) -activation time (min)". For example, 800-20 corresponds with PLWACF prepared by activation at 800 °C for 20 min.

Methods

The porous characteristics of the prepared PLWACF were obtained from nitrogen adsorption/desorption at -196 °C by a surface area analyzer and a pore size analyzer (Quantachrome Instruments). Before each measurement, the samples were degassed at 300 °C for 3 h. The S_{BET} and average pore width were calculated by BET surface area measurement (Brunauer *et al.* 1938). The t-plot micropore analysis method (Deboer *et al.* 1966) was used to calculate the micropore specific surface area (S_{mi}). The total pore volume (V_t) was based on the nitrogen volume adsorbed at the maximum value of relative pressure P/P_0. The density functional theory (DFT) (Lastoskie *et al.* 1993) method was used to calculate the micropore volume (V_{mi}) and mesopore volume (V_{me}). The PSD was also determined according to the DFT method. All the samples were examined for three times and the obtained results are within the accepted error range of 5%.

The burn-off, which is defined as the difference between the mass before and after activation, was calculated as follows,

$$\text{Burn-off} = (w_0\text{-}w_1)/w_0 \times 100\% \quad (1)$$

where w_0 and w_1 are the mass of the carbonized fiber before and after activation, respectively.

RESULTS AND DISCUSSION

Changes of Burn-off

The changes of burn-off by activation at 650 to 800 °C for 20 to 260 min are depicted in Fig. 1 for an exposure interval from 20 to 260 min. As shown, the PLWACF burn-off was increased from 1.75 to 21.03%, 6.90 to 25.96%, 11.03 to 51.2%, and 10.31 to 78.97% as activation period increased from 20 to 260 min by activation at 650, 700,

750, and 800 °C, respectively. According to Fig. 1, the PLWACF seems to be much more reactive at the activation temperature above 750 °C. Such a phenomenon is mainly explained by the increasing rate of reaction between carbon and water steam as the activation temperature increases, which leads to the promotion of the volatilization process (Lua and Guo 2001). Indeed, the water steam is able to penetrate into the solid material and further help in desorption, distillation of the volatiles, and stabilizing the radicals obtained during thermal decomposition, hence resulting in more efficient removal of the volatiles (Minkova *et al.* 2001).

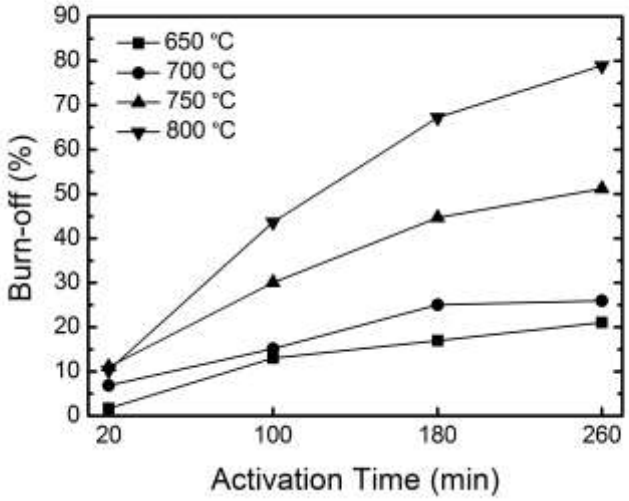

Fig. 1. The changes of burn-off in PLWACF

Pore Structural Evolution

The curves presented in Fig. 2a - d are the typical nitrogen adsorption/desorption isotherms at -196 °C for PLWACF activated for 20 to 260 min at different activation temperatures (600 °C is not included because it is too low to gain an obvious porosity evolution). According to IUPAC classification, all the isotherms exhibit the characteristic of type I (the nitrogen uptake increasing linearly at $P\,P_0^{-1} \leqslant 0.01$), which is ascribable to adsorption on narrow micropores. Meanwhile, the isotherms also exhibit the characteristics of type II (gradient plateaus) and type IV (widening of knees and steeper plateaus) as the activation process proceeding, which is respectively suggestive of the existence of large mesopores (or macropores (with pore width larger than 50 nm)) (Hu *et al*. 2003; Zhang *et al*. 2008) and the formation of mesopores (Lee *et al*. 2003; Zhang *et al*. 2008). The classification of the isotherm type for all the isotherms is presented in Table 1.

Table 1. Classification of the Isotherm Type for the Nitrogen Adsorption/Desorption Isotherms of Prepared PLWACF

Activation Time (min) \ Activation Temperature (°C)	650	700	750	800
20	Type I and II	Type I and II	Type I and II	Type I and II
100	Type I and II	Type I and II	Type I and II	Type I
180	Type I and II	Type I and II	Type I and IV	Type I and IV
260	Type I and II	Type I and II	Type I and IV	Type I and IV

The increase in the PLWACF's nitrogen adsorption capacity became more dependent on the activation time as the activation temperature increased. When activated at 800 °C, the adsorbed volume of nitrogen at $P\ P_0^{-1} \approx 0.99$ was improved by 541 cc g^{-1} with prolonging activation time from 20 to 260 min, reaching a maximum of 822 cc g^{-1} in 800-260.

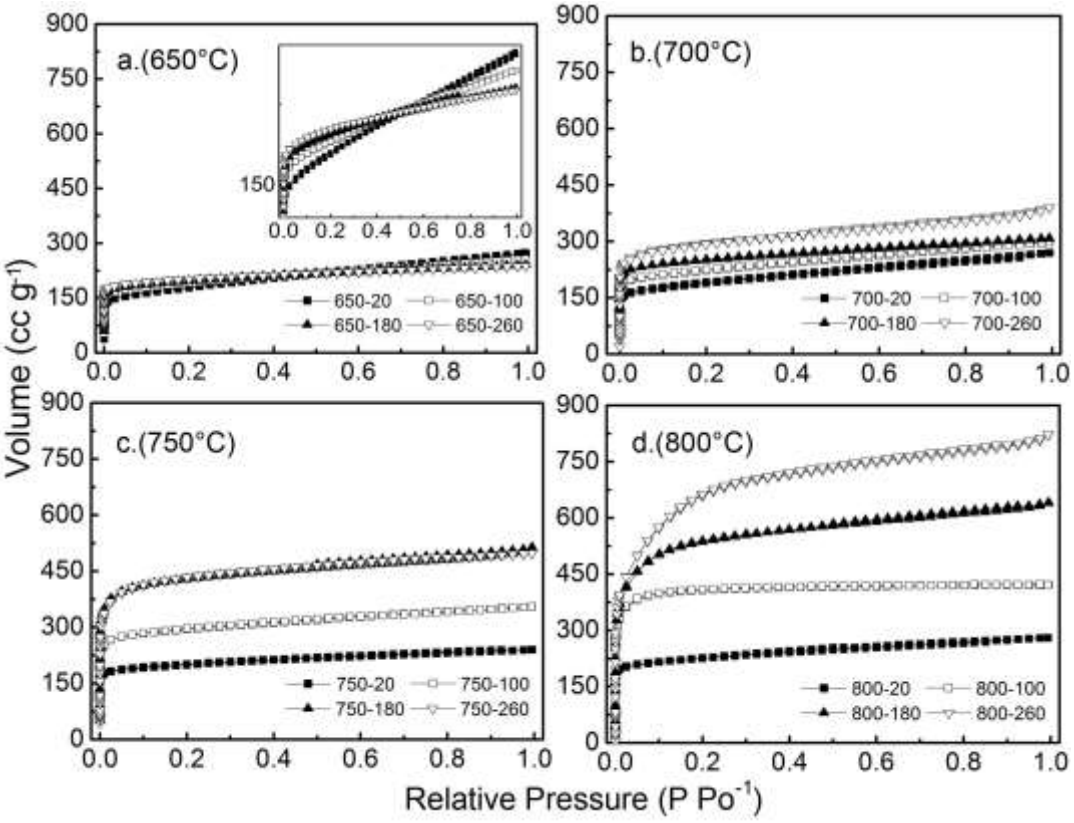

Fig. 2. The nitrogen adsorption/desorption isotherms at -196 °C for the prepared PLWACF. The inset is the partial enlargements of Fig a.

Figure 3 shows the changes of S_{BET} and V_t of PLWACF activated at 650 to 800 °C for 20 to 260 min. As can be seen, the S_{BET} and V_t values were progressively increased with the increase of activation time, and this was more significant with raising activation temperature. The enhancements in S_{BET} by prolonging activation time were from 644 to 785 $m^2\ g^{-1}$, 700 to 1126 $m^2\ g^{-1}$, 776 to 1656 $m^2\ g^{-1}$, and 871 to 2410 $m^2\ g^{-1}$ when activated at 650, 700, 750, and 800 °C, respectively. The V_t was increased by prolonging activation time when the activation temperature was above 700 °C, from 0.417 to 0.604 cc g^{-1} (700 °C), 0.371 to 0.772 cc g^{-1} (750 °C), and 0.434 to 1.272 cc g^{-1} (800 °C). Furthermore, it can be noted that the S_{BET} and V_t were sharply increased with increasing activation time from 20 to 180 min by activation at 750 °C and from 20 to 260 min by activation at 800 °C, which is indicative of the efficient pore formation in PLWACF. These remarkable increases in the S_{BET} and V_t almost followed the same trend as the increase in the burn-off, as shown in Fig. 1, which is mainly due to the enhancement in the reaction activity between carbon and water steam during activation process. Additionally, S_{BET} higher than 1650 $m^2\ g^{-1}$ and V_t larger than 0.800 cc g^{-1} could be obtained only by activation at 800 °C for larger than 100 min.

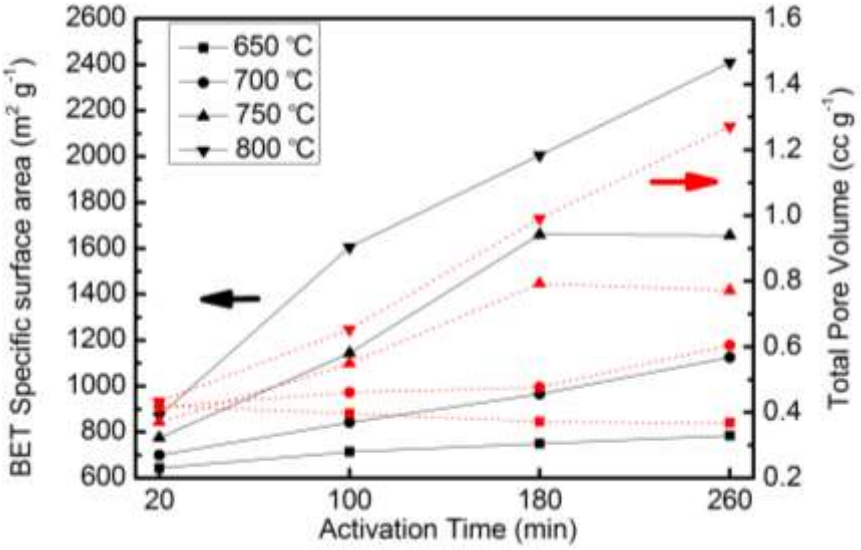

Fig. 3. Changes of BET specific surface area and total pore volume of the prepared PLWACF

Microporosity Evolution

The evolutions of V_{mi} and S_{mi} of PLWACF with activation time when activated at 650, 700, 750, and 800 °C are plotted in Fig. 4. The overall result reveals that microporosity of PLWACF was progressively developed with increasing activation time or activation temperature. The PLWACFs activated at 650 to 700 °C showed a gentle and progressive increase in both the V_{mi} and S_{mi} with increasing activation time in an almost linear fashion. During this process, activation mainly results in the opening of closed pores as well as a deepening and widening the micropores (Jesús Sánchez-Montero *et al*. 2008).

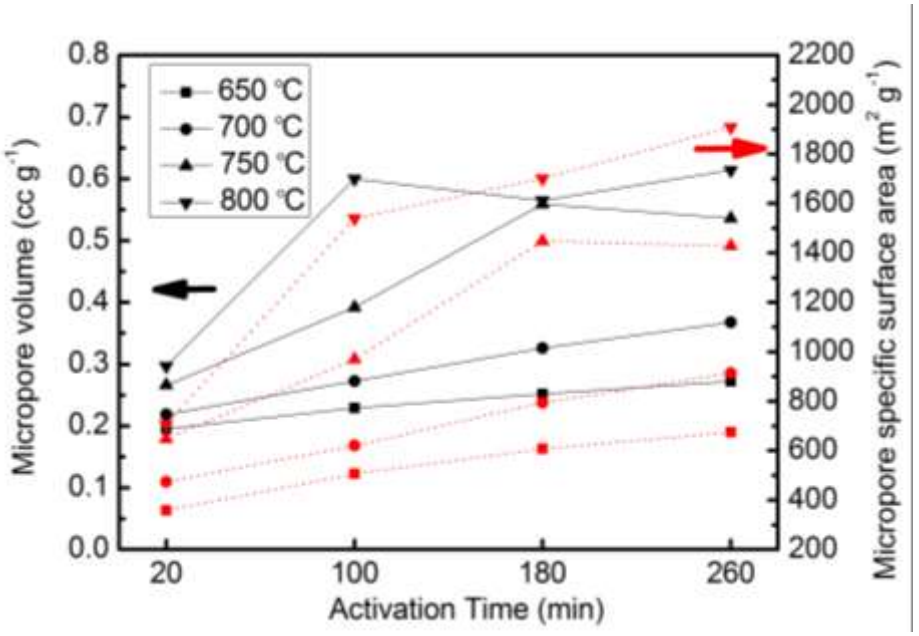

Fig. 4. The evolution of micropore volume and micropore specific surface area of the prepared PLWACF

For PLWACFs activated at 750 to 800 °C, both the V_{mi} and S_{mi} increased sharply as the activation time increased from 20 to 180 min at 750 °C and from 20 to 100 min at 800 °C, suggesting that the breaking through of pore walls begins to be an important mechanism at 750 to 800 °C (Jesús Sánchez-Montero *et al*. 2008). Thereafter, both the V_{mi} and S_{mi} tended to almost stabilize, which can be attributed to the collapse of microporosity as a result of larger activation energy gap (Su *et al.* 2007). On the other hand, the values of both V_{mi} and S_{mi} became greater with a rise of activation temperature throughout the activation time range.

Mesoporosity Evolution

Figure 5 presents the evolutions of V_{me} with activation time for PLWACFs activated at different temperatures. As can be seen, the mesoporosity was not well developed during activation below 800 °C, with the V_{me} values smaller than 0.2 cc g^{-1}. It is worth noting that when activated for 20 to 100 min, higher values of V_{me} were obtained by activation at 650 to 700 °C than at 750 to 800 °C. Because the activation behavior is inclined to generate pores in the original gaps and cracks as well as the non-crystalline region of precursor fiber (Su *et al.* 2012), these higher values of V_{me} may be attributed to the larger original pores and smaller crystallite shape in the precursor fiber carbonized at 650 to 700 °C helping in the removal of carbon and the formation of larger pores (Ma and Zhao 2011; Ma *et al.* 2011). With further activation, the V_{me} tended to decline by activation at 650 to 700 °C, which is likely to have been caused by the carbon structure shrinkage (Aber *et al.* 2009). At activation temperature of 800 °C, the V_{me} was decreased to 0.0 cc g^{-1} with increasing activation time to 100 min, after which it was significantly and proportionally increased to a maximum of 0.545 cc g^{-1} in 800-260. This remarkable increase in the V_{me} was possibly due to the mesoporosity formed through microporosity collapse.

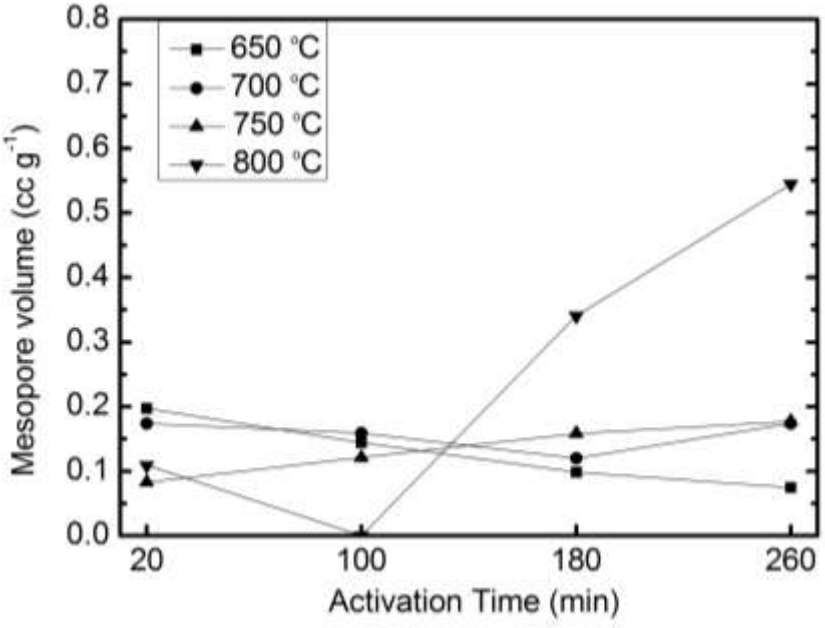

Fig. 5. The evolution of mesopore volume of the prepared PLWACF

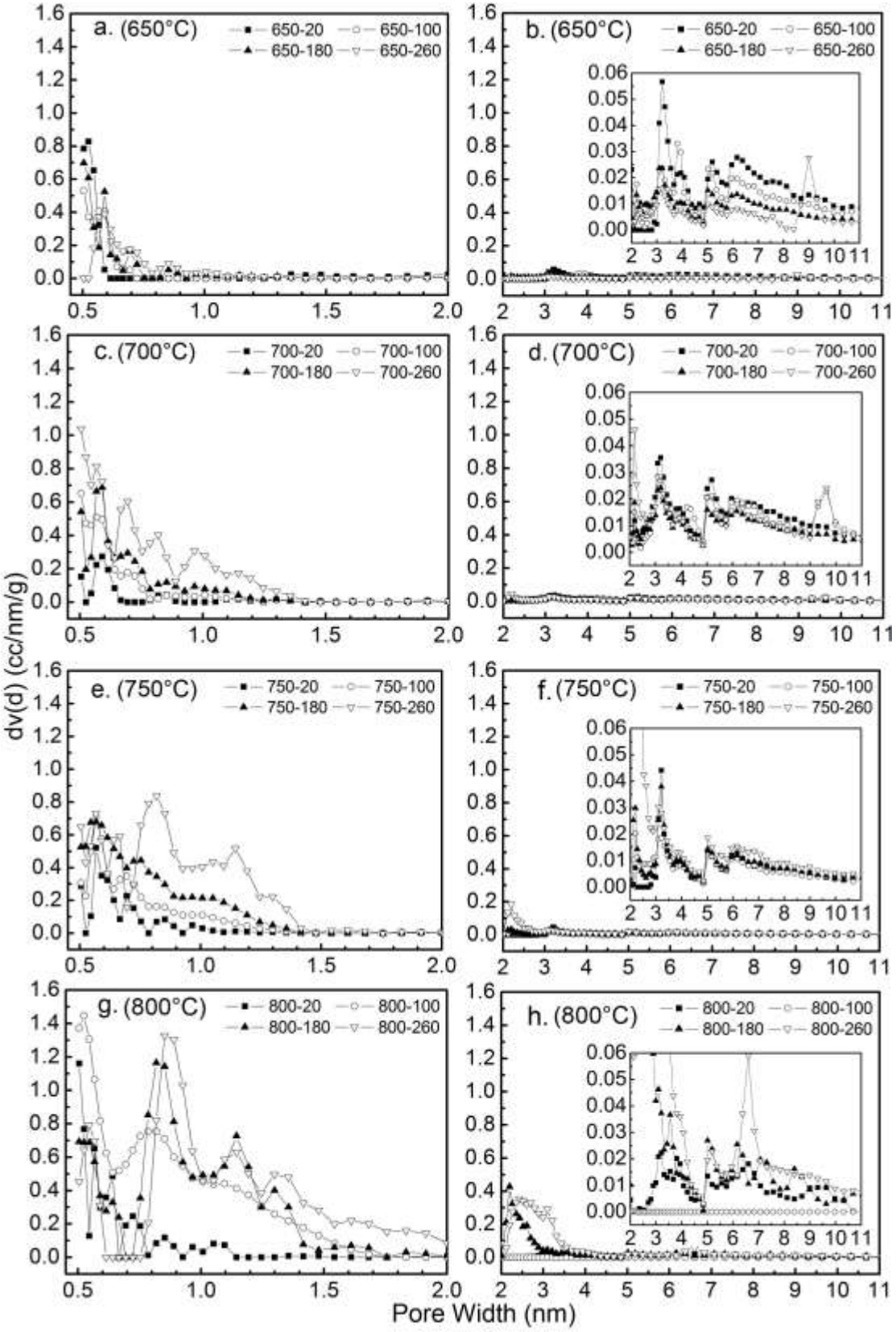

Fig. 6. PSDs obtained for the prepared PLWACFs. The insets are the partial enlargements of Fig. b, d, f, h.

PSD Evolution

The PSDs evolutions of PLWACF with activation time at different activation temperature are presented in Fig. 6. It can be seen that the PSDs of PLWACFs activated at 650 to 700 °C were narrow and confined to a predominance of ultramicropores (with pore width at 0.5 to 0.7 nm) with respect to supermicropores (with pore width at 0.7 to 2 nm), even for long activation time, which makes these materials good candidates for use as molecular sieves (Villar-Rodil *et al*. 2002). The numbers of mesopores formed during activations at 650 to 700 °C are rather small (mainly distributed at 2 to 20 nm with minor yet discernible peaks), which gradually decrease with increasing activation time. When activated at 750 to 800 °C, the PSDs of PLWACFs of 750-20, 750-100, and 800-20 also showed the potential characteristic for molecular sieves. However, the contribution of supermicropores (0.7 to 2 nm) became progressively more important as the activation time increased from 180 to 260 min at 750 °C and from 100 to 260 min at 800 °C, and mesopores mainly at 2 to 4 nm were formed in the cases of 750-260, 800-180, and 800-260, with the amount increasing in the order 800-260 > 800-180 > 750-260. This agrees well with the changes of the average pore width of PLWACF (Table 2), showing that pore widening happened during the late stage of activations at 750 to 800 °C, in a manner that became more significant with increasing activation temperature or time.

Table 2. Changes of the Average Pore Width (nm) of PLWACF

Activation Time (min) \ Activation Temperature (°C)	650	700	750	800
20	0.368	0.368	0.368	0.368
100	0.368	0.368	0.368	0.458
180	0.368	0.368	0.493	0.548
260	0.368	0.368	0.508	0.568

CONCLUSIONS

The porosity evolution of phenol liquefied wood-based activated carbon fiber (PLWACF) with water steam activation at 650 - 800 °C for 20 to 260 min was examined.

1. By the activation processes achieved, the S_{BET} and V_t were increased with the increase of activation time; the effect was most significant with activation at 750 °C for 20 to 180 min and at 800 °C for 20 to 260 min. Combined with the changes of burn-off, it seemed that PLWACF was much more reactive above 750 °C. The S_{BET} higher than 1650 m^2 g^{-1} and V_t larger than 0.800 cc g^{-1} could be obtained only by activation at 800 °C for longer than 100 min. The maximums of S_{BET} and V_t were 2410 m^2 g^{-1} and 1.272 cc g^{-1}, respectively.

2. The microporosity of PLWACF was gently and progressively developed with increasing activation time at 650 to 700 °C, while it was sharply developed at the early stage of activations at 750 to 800 °C, after which it tended to almost become stable, possibly owing to collapse behavior. Furthermore, a higher activation temperature was beneficial for the microporosity development of PLWACF.

3. Higher mesoporosity characteristics were obtained by activation at 650 to 700 °C

than at 750 to 800 °C with activation time from 20 to 100 min. However, the mesoporosity was not well developed during activation below 800 °C. It was significantly developed by activation at 800 °C for longer than 100 min.

4. During activations at 650 to 700 °C, pores of PLWACF that were developed with increasing activation time were principally in the size of ultramicropore range, exhibiting the potential characteristic for molecular sieves. Pore widening happened at the late stage of activations at 750 to 800 °C with supermicropores as well as mesopores (2 to 4 nm) progressively formed.

ACKNOWLEDGMENTS

The authors are grateful for the support of the Special Research Funds of the Forestry Industry for the Public Welfare of China, Grant No. 201004057.

REFERENCES CITED

Aber, S., Khataee, A., and Sheydaei, M. (2009). "Optimization of activated carbon fiber preparation from kenaf using K_2HPO_4 as chemical activator for adsorption of phenolic compounds," *Bioresource Technol*. 100(24), 6586-6591.

Brunauer, S., Emmett, P. H., and Teller, E. (1938). "Adsorption of gases in multimolecular layers," *J. Am. Chem. Soc.* 60(2), 309-319.

Deboer, J. H., Lippens, B. C., Linsen, B. G., Broekhof, J. C., Vandenhe, A., and Osinga, T. J. (1966). "T-curve of multimolecular N_2-adsorption," *J. Colloid and Interface Sci.* 21(4), 405-411.

Hu, Z. H., Guo, H. M., Srinivasan, M. P., and Ni, Y. M. (2003). "A simple method for developing mesoporosity in activated carbon," *Sep. Purif. Technol.* 31(1), 47-52.

Im, J. S., Jung, M. J., and Lee, Y. S. (2009). "Effects of fluorination modification on pore size controlled electrospun activated carbon fibers for high capacity methane storage," *J. Colloid and Interface Sci.* 339(1), 31-35.

Jesús Sánchez-Montero, M., Salvador, F., and Izquierdo, C. (2008) "Reactivity and porosity of a carbon fiber activated with supercritical CO_2," *J. Phys. Chem. C*. 112 (13), 4991-4999.

Konwar, R. J., and De, M. (2013). "Effects of synthesis parameters on zeolite templated carbon for hydrogen storage application," *Micropor. Mesopor. Mat.* 175(15), 16-24.

Kumar, K., Kothari, R., and Bohra, J. N. (1997). "Effect of reactive atmosphere and maximum heat treatment temperature on char characteristics of pyrolyzed rayon cloth," *Carbon* 35(5), 703-706.

Lastoskie, C., Gubbins, K. E., and Quirke, N. (1993). "Pore-size distribution analysis of microporous carbons - A density-functional theory approach," *J. Phys. Chem.* 97(18), 4786-4796.

Lee, Y. S., Basova, Y. V., Edie, D. D., Reid, L. K., Newcombe, S. R., and Ryu, S. K. (2003). "Preparation and characterization of trilobal activated carbon fibers," *Carbon* 41(13), 2573-2584.

Liu, W., and Zhao, G. (2012). "Effect of temperature and time on microstructure and surface functional groups of activated carbon fibers prepared from liquefied wood,"

BioResources 7(4), 5552-5567.
Lua, A. C., and Guo, J. (2001). "Preparation and characterization of activated carbons from oil-palm stones for gas-phase adsorption," *Colloids Surf. A* 179(2-3), 151-162.
Ma, X., and Zhao, G. (2011). "Variations in the microstructure of carbon fibers prepared from liquefied wood during carbonization," *J. Appl. Polym. Sci.* 121(6), 3525-3530.
Ma, X., Zhao, G., Liu, X., and Yu, L. (2011). "Effects of carbonization temperatures on the adsorption properties and pore structure of carbon fibers from liquefied wood," *J. Func. Mater.* 42(10), 1746-1749.
Minkova, V., Razvigorova, M., Bjornbom, E., Zanzi, R., Budinova, T., and Petrov, N. (2001) "Effect of water vapour and biomass nature on the yield and quality of the pyrolysis products from biomass," *Fuel Process. Technol*. 70(1), 53-61.
Naik, J. R., Bikshapathi, M., Singh, R. K., Sharma, A., Verma, N., Joshi, H. C., and Srivastava, A. (2011). "Preparation, surface functionalization, and characterization of carbon micro fibers for adsorption applications," *Environ. Eng. Sci.* 28(10), 725-733.
Osmond, N. M. (2000). "Activated carbon fibre adsorbent materials," *Adsorpt. Sci. Technol.* 18(6), 529-539.
Qiao, W. M., Huda, M., Song, Y., Yoon, S. H., Korai, Y., Mochida, I., Katou, O., Hayashi, H., and Kawamoto, K. (2005). "Carbon fibers and films based on biomass resins," *Energ. Fuel.* 19(6), 2576-2582.
Su, C. I., and Wang, C. L. (2007). "Optimum manufacturing conditions of activated carbon fiber absorbents. I. Effect of flame retardant reagent concentration," *Fibers Polym.* 8(5), 477-481.
Su, C. I., Zeng, Z. L., Peng, C. C., and Lu, C. H. (2012). "Effect of temperature and activators on the characteristics of activated carbon fibers prepared from viscose-rayon knitted fabrics," *Fibers Polym.* 13(1), 21-27.
Uraki, Y., Kubo, S., Kurakami, H., and Sano, Y. (1997). "Activated carbon fibers from acetic acid lignin," *Holzforschung* 51(2), 188-192.
Uraki, Y., Nakatani, A., Kubo, S., and Sano, Y. (2001). "Preparation of activated carbon fibers with large specific surface area from softwood acetic acid lignin," *J. Wood Sci.* 47(6), 465-469.
Villar-Rodil, S., Denoyel, R., Rouquerol, J., Martínez-Alons, A., Tascón, J. M. D. (2002). "Porous texture evolution in nomex-derived activated carbon fibers," *J. Colloid Interface Sci*. 252(1), 169-176.
Xu, B., Wu, F., Chen, R., Cao, G., Chen, S., and Yang, Y. (2010). "Mesoporous activated carbon fiber as electrode material for high-performance electrochemical double layer capacitors with ionic liquid electrolyte," *J. Power Sources* 195(7), 2118-2124.
Xie, J. C., Wang, X. H., and Deng, J. Y. (2004). "Modifying the pore structure of pit-ACF with the chemical vapor deposition of methane and propylene," *Micropor. Mesopor. Mat.* 76(1-3), 167-175.
Yang, M. C., and Yu, D. G. (1998). "Influence of activation temperature on the properties of polyacrylonitrile-based activated carbon hollow fiber," *J. Appl. Polym. Sci.* 68(8), 1331-1336.
Zhang, S. J., Feng, H. M., Wang, J. P., and Yu, H. Q. (2008). "Structure evolution and optimization in the fabrication of PVA-based activated carbon fibers," *J. Colloid and Interface Sci.* 321(1), 96-102.

Article submitted: Dec. 5, 2014; Peer review completed: Jan. 29, 2014; Revised version received: Feb. 26, 2014; Accepted: March 2, 2014; Published: March 5, 2014.